Error Analysis in Laser Vibrometer Measurements of Lamb Waves

M. N. NEUMANN and R. LAMMERING

ABSTRACT

Lamb waves are widely employed for structural health monitoring in thin plate structures by interpreting their interaction with damages. For the observation of Lamb waves, scanning laser vibrometry is a common technique providing spatial and temporal information on the wave field. One-dimensional scanning vibrometry, due to its lower costs, is more spread than 3D vibrometry, but generates systematic errors measuring oblique-angled vibrations. This is owing to the physical principle of the technique: The directly measured value is the projection of the actual vibration velocity vector to the laser beam containing no information on the direction, hence, any angle other than zero between beam and velocity vector produces a significant error, which, with knowledge of the angle, may be corrected afterwards. Measuring lamb wave fields, the velocity vector rotates with the angular frequency of the excitation. For transient experiments on finite-size plates, the actual angle is undetermined. Thus, the induced error is not correctable. In addition to the error in amplitude, the association of phase and vibration direction induces an error concerning the observed phase velocity and hence a seeming phase shift. The quantity of both, amplitude and phase error is shown and a workaround to avoid them is deduced. Three-dimensional data sets are, of course, free of the mentioned errors, so a method to perform 3D-Scans employing 1D-hardware is deduced and presented.

INTRODUCTION

Ultrasonic Lamb waves are a promising phenomenon for Structural Health Monitoring purposes for their visible interaction with discontinuities in thin-walled structures. After excitation by, for example, a piezoceramic wafer under alternating

Mirko Nikolaj Neumann, Rolf Lammering
Helmut-Schmidt-Universität, Universität der Bundeswehr Hamburg
Fakultät für Maschinenbau, Institut für Mechanik
Holstenhofweg 85, D-22043 Hamburg
mirko.neumann@hsu-hh.de

current, the wavefield is disturbed at locations of structural inhomogeneities, as damages.

A common method for quasi-continuous observation in both time and space is scanning laser vibrometry, quickly providing experimental results without retroaction to the structure. For many applications, like vibrations of two-dimensional structures, one-dimensionally working equipment does fine. Three-dimensional devices come along with vastly higher costs, why most researchers are bound to employ standard-, one-dimensional vibrometers.

The severe disadvantage is that the trajectories of Lamb waves are no straight oscillations but the material points move in ellipses. These are far from comparability to straight, thus correct information on particle motion and the resulting wave fields can only be obtained performing 3D-experiments.

This work deduces the caused errors both in time and phase quantitavely and presents a workaround to obtained three-dimensional information employing one-dimensional equipment.

ONE-DIMENSIONAL OBSERVATION OF OBLIQUE-ANGLED MOTION

Laser vibrometry

Laser (Doppler-) vibrometry measures oscillation velocities along the laser beam by means of the optical Doppler shift.

The split up laser beam is partly projected to the object and recombined with the reference beam on an interferometer. The resulting beat frequency is measured and directly proportional to the signless oscillation velocity. The sign is reproduced by shifting the reference beam's frequency through a bragg cell, cf. [1].

Scanning vibrometers repeat the measurement at all defined grid points. At each point the experiment is repeated with unchanged parameters and all single time series are combined to a video-like representation of the data, discretised by sampling frequency and grid increments.

Axis-parallel oscillation

Conventional (1D-) scanning vibrometers work under the assumption of motion parallel to the non-deflected measurement beam, which may be considered the *z*-axis. This way, the only component of an oscillator's velocity vector is $v_z = v = |\mathbf{v}|$.

Since vibrometers generally measure the velocity component in the beam direction – the projection of the velocity vector to the beam (angle α) – the caused error can be compensated via $v_{meas1\mathrm{d}} = v_z \cos\alpha$, cf. Figure 1, left.

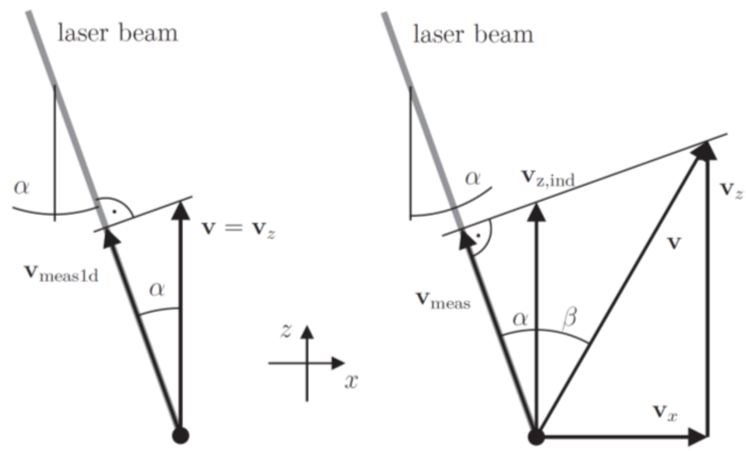

Figure 1: Axis-parallel (left) and oblique-angled oscillation (right, angle β) under observation by a deflected measurement beam (angle α)

Oblique-angled oscillation

For oscillations not parallel, but under some arbitrary angle to the *z*-axis (angle β, see figure 1 right), the above mentioned error compensation cannot work properly. Again, the measured velocity is the projection of the velocity vector to the beam, i.e. $v_{meas} = v\cos(\alpha+\beta)$. The angle compensation of the used vibrometry software gives the value $v_{z,ind} = v_{meas}/\cos\alpha$, while the correct out-of-plane velocity is $v_z = v\cos\beta$. This yields the relative error factor

$$\frac{v_{z,ind}}{v_z} = \frac{\cos(\alpha+\beta)}{\cos\alpha\cos\beta} = 1 - \tan\alpha\tan\beta. \tag{1}$$

Clearly for at least one angle equal zero, either vertical laser beam or oscillation, there is no error. For any angle equal 90°, the error becomes infinite. For technical reasons, α can not be 90°, whereas β, in the case of elliptic trajectories of particle motion, reaches ±90° twice every period.
The error may be decreased by deactivating angle-compensating measures, then it becomes

$$\frac{v_{meas}}{v_z} = \frac{\cos(\alpha+\beta)}{\cos\beta} \tag{2}$$

This results in a somewhat smaller error, which is nevertheless of inacceptable quantity making the *results unsuitable for quantitative evaluation*.

OBSERVATION OF LAMB WAVES USING 1D-VIBROMETRY

With the oscillators (material points) travelling along the mentioned elliptic trajectories, the angle β (movement direction) is no longer constant but time-variant.

Lamb waves, simplified plate wave approach

To keep things short, Lamb waves deduced from mathematics of continuum mechanics will be skipped here. See, e.g., [3] for detailed explanations.

Not considering the investigated structure as a three-dimensional continuum but modeling it as a (Kirchhoff-) plate for flexural waves (analogue to A_0 Lamb waves) and as a plate under plane stress for pressure waves (analogue to S_0 Lamb waves) simplifies the proceeding significantly.

The simplification gives very good results for "low" frequencies, which are the technically most relevant ones. Phase velocities of the flexural waves c_F and of the pressure wave c_P are then determined by

$$c_F = \sqrt[4]{\frac{E}{12\rho\left(1-\nu^2\right)}}\sqrt{\omega h} \text{ and } c_P = \sqrt{\frac{1}{1-\nu^2}\frac{E}{\rho}} \tag{5}$$

with plate thickness h, Young's modulus E, density ρ and the Poisson ratio ν at an angular frequency ω.

Detailed derivations of (5) may be found e.g. in [4].

The displacement (u and w for for displacements in x- and z-direction, cf. Figure 2) field of such waves (travelling in positive x-direction) *at the upper (measurable) plate surface* is described by

$$u_F = \tfrac{1}{2}h \cdot w_{0F} \cdot k \cdot \cos\left(\omega t - kx\right) \text{ ,} \tag{6}$$

$$w_F = w_{0F} \cdot \sin\left(\omega t - kx\right) \text{ ,} \tag{7}$$

$$u_P = u_{0P} \cdot \cos\left(-\omega t - kx\right) \text{ and} \tag{8}$$

$$w_P = -\tfrac{1}{2}h \cdot \tfrac{\nu}{\nu-1} \cdot k \cdot u_{0P} \cdot \sin\left(-\omega t - kx\right) \text{ [1].} \tag{9}$$

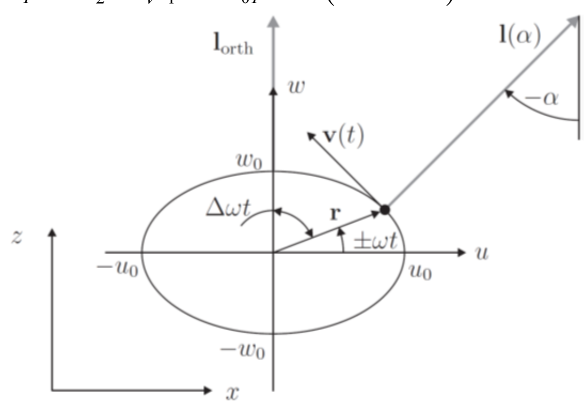

Figure 2: Elliptical trajectory of particle motion for orthogonal and oblique-angled measurement

The ratios of out-of-plane- to in-plane-amplitude, i.e., the ellipses shapes, can so be determined as

$$\left(\tfrac{w_0}{u_0}\right)_F = 2\left(hk\right)^{-1} \text{ and} \tag{10}$$

$$\left(\tfrac{w_0}{u_0}\right)_P = \tfrac{1}{2}hk\tfrac{\nu}{\nu-1} \text{ .} \tag{11}$$

Phase shift errors in 1D vibrometer scans

The displacement velocity vector field of plate waves is the time derivative of equations (6-9):

$$\partial u_F / \partial t = -\tfrac{1}{2}h \cdot k \cdot w_{0F} \cdot \omega \cdot \sin\left(\omega t - kx\right) \text{ ,} \tag{12}$$

---

[1] The negative sign for equation (9) results from the clockwise spin direction of symmetric Lamb waves here.

$$\partial w_F / \partial t = w_{0F} \cdot \omega \cdot \cos(\omega t - kx) \ , \tag{13}$$

$$\partial u_P / \partial t = -u_{0P} \cdot \omega \cdot \sin(\omega t - kx) \text{ and} \tag{14}$$

$$\partial w_P / \partial t = -\tfrac{1}{2} h \cdot k \cdot \tfrac{\nu}{\nu - 1} u_{0P} \cdot \omega \cdot \cos(\omega t - kx) \ . \tag{15}$$

The measured signal reaches zero when oscillation and laser beam are orthogonal to each other: $\mathbf{v} \cdot \mathbf{l}(\alpha) = 0$. Here,

$$\mathbf{v} = \begin{pmatrix} \partial u / \partial t \\ 0 \\ \partial w / \partial t \end{pmatrix} \text{ and } \mathbf{l} = \alpha \begin{pmatrix} \sin(-\alpha) \\ 0 \\ \cos(-\alpha) \end{pmatrix} , \tag{16}$$

where, after normalizing both vectors to

$$\mathbf{e}_v = \begin{pmatrix} v_x / |\mathbf{v}| \\ 0 \\ v_z / |\mathbf{v}| \end{pmatrix} \text{ and } \mathbf{e}_l = \begin{pmatrix} \sin(-\alpha) \\ 0 \\ \cos(-\alpha) \end{pmatrix} , \tag{17}$$

orthogonality is expressed as negative, reciprocal slope,

$$\begin{pmatrix} e_{\upsilon x} \\ 0 \\ e_{\upsilon z} \end{pmatrix} = \begin{pmatrix} e_{lz} \\ 0 \\ -e_{lx} \end{pmatrix} . \tag{18}$$

ωt is separated from one scalar component of (18). The conclusion $\Delta\omega t = \frac{\pi}{2} - \omega t$ (see Figure 2) yields the shift in phase of actual to measured out-of-plane displacement (velocity) field

$$\Delta\omega t = \frac{\pi}{2} - \arccos \sqrt{\frac{1 - \cos^2 \alpha}{1 - \cos^2 \alpha \left(1 - \left(\frac{w_0}{u_0}\right)^2\right)}} \ . \tag{19}$$

Knowing that $\frac{\Delta\omega t}{2\pi} = \frac{\Delta x_{phase}}{\lambda}$ allows the more illustrative expression

$$\frac{\Delta x_{phase}}{\lambda} = \frac{1}{4} - \frac{1}{2\pi} \arccos \sqrt{\frac{1 - \cos^2 \alpha}{1 - \cos^2 \alpha \left(1 - \left(\frac{w_0}{u_0}\right)^2\right)}} \ . \tag{20}$$

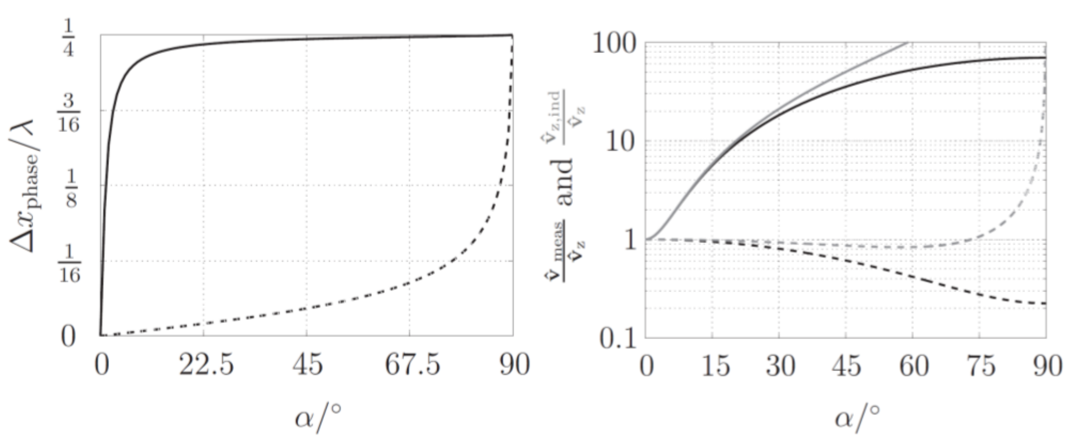

Figure 3: Relative phase (left) and amplitude error (right) wrongly observed with 1D scanning vibrometry plotted over scanning angle α. Solid: Symmetric modes, dash-dotted: antisymmetric modes. Grey: Active software-sided angle compensation.

The relative phase shift (20) is plotted over the scanning angle α in Figure 3 left.

It is obvious that measured symmetric waves are weighted by enormous *phase errors (up to about a quarter wavelength)*, while the influence on antisymmetric wave observation is relatively small within the technically relevant angles (up to about 25°).

Amplitude errors observing Lamb waves with 1D-vibrometry

The error quantity of out-of-plane oscillations measured with an oblique-angled laser beam is described by (1), respectively (2). With the rotating oscillation vector of waves, this error reaches infinity twice per period and is hence not very useful for a description in this matter.

A comparison of the actual amplitude $\hat{v}_{\text{meas}}$ and the measured amplitude $\hat{v}_z$ of the velocities is more helpful. The measured quantity is the projection of the displacement velocity vector to the laser beam:

$$v_{\text{meas}} = \mathbf{v} \cdot \mathbf{e}_l \tag{21}$$

$$= \begin{pmatrix} -u_0 \cdot \omega \cdot \sin(\omega t) \\ 0 \\ w_0 \cdot \omega \cdot \cos(\omega t) \end{pmatrix} \cdot \begin{pmatrix} \sin\alpha \\ 0 \\ \cos\alpha \end{pmatrix} \tag{22}$$

$$= u_0 \cdot \omega \cdot \sin(\omega t)\sin\alpha + w_0 \cdot \omega \cdot \cos(\omega t)\cos\alpha \tag{23}$$

The sought extremum is found at the root of both partial derivatives

$$\partial v_{\text{meas}} / \partial t = u_0 \cdot \omega^2 \cdot \cos(\omega t)\sin\alpha - w_0 \cdot \omega^2 \cdot \sin(\omega t)\cos\alpha$$

and

$$\partial v_{\text{meas}} / \partial \alpha = u_0 \cdot \omega \cdot \sin(\omega t)\cos\alpha - w_0 \cdot \omega \cdot \cos(\omega t)\sin\alpha \tag{25}$$

(24)

yielding $\omega t=\alpha$. Hence, the measured amplitude

$$\hat{v}_{\text{meas}} = v_{\text{meas}}(\omega t = \alpha) \tag{26}$$

$$= u_0 \cdot \omega \cdot \sin^2\alpha + w_0 \cdot \omega \cdot \cos^2\alpha \tag{27}$$

The error factor is the quotient of (27) and the actual out-of-plane velocity $\hat{v}_z$:

$$\tfrac{\hat{v}_{\text{meas}}}{\hat{v}_z} = \tfrac{u_0}{w_0}\sin^2\alpha + \cos^2\alpha \ , \tag{28}$$

converging to $\tfrac{u_0}{w_0}$ for α=90°

Figure 3, right hand side, depicts the relative amplitude error plotted over the scanning angle α, evincing the enlarged error quantity diverging to infinity with active vibrometer-sided angle compensation described by

$$\tfrac{\hat{v}_{z,\text{ind}}}{\hat{v}_z} = \cos^{-1}\alpha \cdot \left(\tfrac{u_0}{w_0}\sin^2\alpha + \cos^2\alpha\right) \tag{29}$$

Vibrometric area scans

The most common application for scanning vibrometry is the scanning of areal surfaces. In this case the waves are not generally travelling towards or away from the point of normality between surface and laser beam.

The distribution of phase- and amplitude errors for a specific experiment is shown in figure 4. The experiment was repeated with identical parameters: Transient excitation of waves at the center of a quadratic plate.

The first measurement (right) was made with a vertically mounted scanning head – the error is distributed uniformly outwards from the wave source and hence not visible.
The second measurement was performed with the scanning head on a tripod, the non-deflected laser beam at a degree of about 45° to the plate surface. The amplitude error is larger and clearly variable with respect to the area. The phase shift is large and changes sign at the black sketched lines, where the influence of the in-plane velocity component on the measured signal vanishes: $\mathbf{v}_z \cdot \mathbf{e}_l = 0$, cf. eqs. (21) to (23).

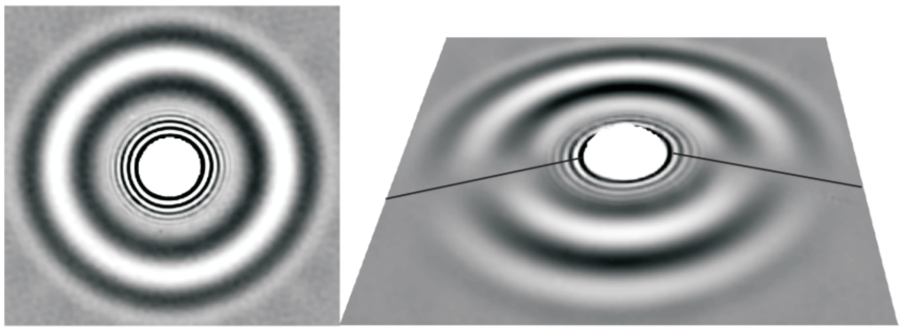

Figure 4: "Out-of-plane" velocity field from 1D measurement of transiently excited Lamb waves in a plate. Left: Undeflected laser beam orthogonal to plate surface. Right: Undeflected beam 45° to plate surface.

AVOIDANCE OF SYSTEMATIC ERRORS OBSERVING OBLIQUE-ANGLED OSCILLATIONS

The formerly discussed errors can be critical, when quantitative data is needed for runtime measurements, comparison to computationally obtained data and other purposes.
One option to obtain correct data is single-point-measuring with a vertical measurement beam, not allowing area scans.
3D scanning vibrometry avoids the problems by producing data in a cartesian system, clearly separating the components in different spatial directions.
Because commercial 3D vibrometer systems are connected to about triple the costs of standard 1D systems, many researchers are bound to the latter.
An approach requiring a higher time effort but keeping the investment in equipment short, is the combination of three independent 1D scans from different directions into the sought 3D wave field.
A comprehensive description of such a technique is given in [5].

Figure 5 shows the actual fields of view of three 1D scans, all of them observing the same, repeated experiment from different directions.

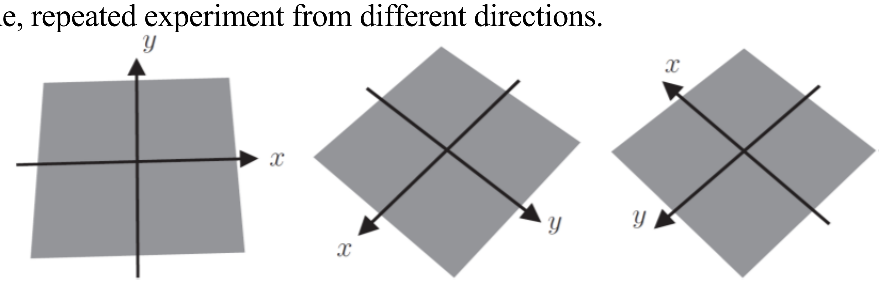

Figure 5: Views of a scanned area from different measuring directions

Surface plots of the separate Cartesian components resulting from the transformation of these measurements are given in Figure 6.

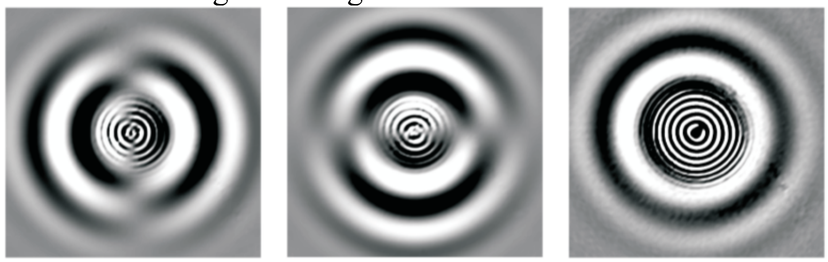

Figure 6: Snapshots of *x*-, *y*- and *z* displacement field of Lamb waves after transient excitation.

CONCLUSIONS

The paper shows systematic measurement errors, which generally occur in observation of oblique-angled oscillations with 1D scanning laser vibrometry.
The errors were quantified and, with special focus on Lamb waves, different error qualities for amplitude and phase, deduced and also determined in size.

Knowledge about these error influences on experimentally obtained data can help understanding deviations between simulation and experiment. Subjective errors in past comparisons of both can possibly be neglected afterwards.

For future wave – or oscillation in general – observation a deliberate decision whether the precision of 3D scanning is necessary or not, can be made and, if so, a workaround for 3D scanning with 1D equipment (see[5]) can be employed.

ACKNOWLEDGEMENTS

The financial support of the Deutsche Forschungsgemeinschaft is gratefully acknowledged.

REFERENCES

1. Axel Donges and Reinhard Noll. *Lasermeßtechnik: Grundlagen und Anwendungen*. Hüthig Buch Verlag GmbH, Heidelberg, 1993.
2. Horace Lamb. On waves in an elastic plate. In *Proceedings of the Royal Society of London Series A, Vol. XCIII*, pages 114–128, 1917.
3. Karl F. Graff. *Wave Motion in Elastic Solids*. Oxford University Press, 1975. Dover edition, Dover Publications, Inc., New York, 1991.
4. Victor Giurgiutiu. *Structural health monitoring with piezoelectric wafer active sensors*. Elsevier Inc., Burlington, USA, 2008.
5. Mirko Nikolaj Neumann, Bianca Hennings, and Rolf Lammering (2012). *Identification and avoidance of systematic measurement errors in Lamb wave observation with 1d scanning laser vibrometry.* Manuscript submitted for publication.